Antiresonances in the excitation and absorption spectra of Cr^{3+}-doped fluoride glasses

M. A. Illarramendi, R. Balda, and J. Fernández
Departamento de Física Aplicada I, Escuela Técnica Superior de Ingenieros Industriales y de Telecommunicación, Universidad del País Vasco, Alameda de Urquijo s/n 48013 Bilbao, Spain
(Received 7 August 1992; revised manuscript received 4 January 1993)

Absorption and excitation spectra of Cr^{3+}-doped fluoride glasses exhibit features that can be interpreted as Fano antiresonance lines due to interactions between the ^2E, $^2T_1$ sharp levels and the vibrationally broadened $^4T_2$ quasicontinuum. A study of the influence of glass inhomogeneity on the antiresonance profiles of Cr^{3+} time-resolved laser-excitation spectra at 4.2 K was performed for four fluoride glasses. The Fano theory adapted by Sturge, Guggenheim, and Pryce has also been used to develop a method to analyze the change of the resonance-line-shape parameter q as a function of the peak position and half width of the background absorption spectrum. The analysis includes background spectra consisting of a single- and a double-Gaussian function. A qualitatively good agreement with the experimental data for several fluoride glasses has been obtained.

I. INTRODUCTION

The optical properties of Cr^{3+}-doped glasses have attracted much attention over the past few years.[1–10] In most instances the crystalline-field strength of the host environment is weak and a large vibronically broadened $^4T_2 \rightarrow {}^4A_2$ emission occurs. Moreover, the inherent disorder of the glass structure gives a broad distribution of field strengths, and a site-to-site variation in oscillator strengths results, giving additional inhomogeneous broadening even at the lowest temperatures.[11] In spite of the expected sensitivity to variations of the local Cr^{3+} environments, the main features of the absorption spectra of Cr^{3+} in various glasses are only slightly influence by the composition of the glass host.[12] The Cr^{3+} spectra are dominated by the local bonding at the Cr^{3+} site as can be understood by assuming that, on the average, the chromium ions occupy sites that have nearly octahedral symmetry. This configuration is dominant because the strong ligand field stabilization energy of Cr^{3+} in a sixfold coordination. It is well known that parity-forbidden *d-d* excitations in transition-metal ions can be partially allowed if cubic symmetry is slightly distorted by the presence of a weak low-symmetry field of odd parity or if it is instantaneously distorted by the presence of odd-parity molecular vibrations. In the latter case, it can be proved[13] that absorption oscillator strength values are independent of the form of the excited-state potential-energy curve even if the excited state involves a change in geometry, force constant, or anharmonicity with respect to the odd-parity nuclear coordinates. Therefore, the energy levels observed in the absorption and emission spectra are usually interpreted by the Tanabe-Sugano diagram for d^3 systems with octahedral coordination.[4,14,15]

In a previous work[16] the authors analyzed the features of the long-wavelength $^4A_2 \rightarrow {}^4T_2$ absorption spectra in several heavy-metal and transition-metal fluoride glasses in terms of an interaction between the intra t^3 levels (^2E, $^2T_1$) and the vibronically broadened t^2e level ($^4T_2$) resulting in Fano-type antiresonances.[17,18] These features are similar to those observed in $KMgF_3:V^{2+}$ by Sturge, Guggenheim, and Pryce,[19] in Cr^{3+}-doped nonfluoride glasses by Lempicki *et al.*,[20] and more recently in the excitation spectra of divalent europium by Meijerink and Blasse.[21] The values obtained for the parameters involved in our model were well in accordance with the structural and spectroscopic data.[7–10]

The aim of this work is to analyze the influence of glass inhomogeneity on the antiresonance lines observed in Ref. 16. As far as we know the influence of inhomogeneous broadening on the Fano antiresonance profiles has not been studied, although it has been invoked to explain both the displacement of the ^2E level due to the coupling with the continuum and the increasing of the linewidth in nonfluoride glasses.[20] To see these effects, we performed time-resolved (TR) luminescence excitation spectra at 4.2 K for Cr^{3+} in several heavy-metal fluoride glasses (HMFG), monitored at different emission wavelengths (λ_{em}) which were subsequently analyzed in the framework of Fano's theory. To study the change of the antiresonance profiles as a function of the parameters related to the background absorption spectrum (peak position and half-width), we have developed a method based on the Fano theory as adapted by Sturge, Guggenheim, and Pryce.[19] The analysis has been performed taking for the background a single- and a double-Gaussian function. Although the effect of the Cr^{3+} site distributions on the experimental absorption profile would be better accounted for by using a double-Gaussian function, a qualitative good agreement with experimental data reported in Ref. 16 was obtained by a single-Gaussian background function.

II. THEORETICAL GROUNDS

The antiresonance profiles are analyzed in terms of the ratio $R(E)$ of the observed absorption profile to the background given by Fano's theory[17,18] as

$$R(E)=1+\sum_i \rho_i^2 \frac{\gamma_i^2 q_i^2-\gamma_i^2+2q_i\gamma_i(E-E_{ri})}{\gamma_i^2+(E-E_{ri})^2}\ , \quad (1)$$

where

$$\rho_i=\langle \Psi_{Ei}^{(a)}|\Psi_{Ei}^{(d)}\rangle,\ \ \rho_i^2\le 1\ , \quad (2)$$

$$\gamma_i=\pi\langle \Psi_{Ei}^{(a)}|H_i|\varphi_i\rangle^2, \quad (3)$$

$$q_i=\frac{\langle \Phi_i|z|\Psi_0\rangle}{\sqrt{\pi\gamma_i}\rho_i\langle \Psi_{Ei}^{(d)}|z|\Psi_0\rangle}\ . \quad (4)$$

Index i ranges over the number of sharp levels. ρ_i^2 is the overlap integral of $\Psi_{E_i}^{(a)}$ and $\Psi_{E_i}^{(d)}$ which arise, respectively, by autoionization of φ_i and by direct transition from ground state Ψ_0. γ_i indicates the spectral width of the autoionized state φ_i. The interaction Hamiltonian H_i connects the sharp excited state φ_i to a certain fraction of the continuum $\Psi_{E_i}^{(a)}$. For the Cr^{3+} ion, the interaction mechanism is the spin-orbit coupling. q_i is a numerical index which characterizes the line profile. It is related to the transition dipole matrix elements for the modified sharp level Φ_i and the broad states. E_{r_i} is the resonance energy which is slightly shifted due to the interaction with the continuum, compared to the resonance energy for the unperturbed sharp absorption line.

There exists an independent method for calculating q_i and γ_i using the Fano theory adapted by Sturge, Guggenheim, and Pryce.[19] In particular, the values for q can be calculated from the Hilbert transform of the background spectrum $G_2(E)$:

$$q=\frac{(1/\pi)P\int_{-\infty}^{+\infty}[G_2(E)dE/(E_0-E)]}{G_2(E_0)}\ , \quad (5)$$

where P denotes the Cauchy principal value of the integral and E_0 is the resonance frequency for the unperturbed sharp absorption line.

III. EXPERIMENTAL TECHNIQUES

The fluoride glasses used in this study were prepared at the Mineral Chemistry Laboratory of the Rennes University (France). The molar composition of the six fluoride glasses used in this study are described in Table I. The samples were doped with 0.5 mol% Cr^{3+}. The experimental method for preparing the glass has been well described in the literature.[22,23] Briefly, after fluorination of the starting oxide materials at 350 °C, the mixture is melted under a controlled atmosphere. Then the melt is poured into a brass mold and annealed at a temperature slightly above the glass temperature, T_g. Finally, the samples are cut and polished for optical measurements.

The sample temperature was varied between 4.2 and 300 K with a continuous-flow cryostat. Conventional absorption spectra were performed with a CARY 17 spectrophotometer. The excitation spectra were obtained by exciting the sample with a tunable dye laser (1-ns pulse width). The fluorescence was analyzed using a 0.22-m SPEX monochromator and detected by a Hamamatsu R7102 extended ir photomultiplier. The spectra were processed by a 4400 EGG-PAR boxcar integrator and corrected by taking into account the profile of DCM dye.

TABLE I. Chemical composition of glasses used in this work.

Glass	Composition in mole percent
ZBL	$62ZrF_4$-$30BaF_2$-$8LaF_3$
ZBLA	$57ZrF_4$-$34BaF_2$-$4.5LaF_3$-$4AlF_3$
ZBLAN	$58ZrF_4$-$18BaF_2$-$5.5LaF_3$-$3AlF_3$-15NaF
BIZYT	$30BaF_2$-$30InF_3$-$20ZnF_3$-$10YF_3$-$10ThF_4$
BIGaZYT1	$30BaF_2$-$18InF_3$-$12GaF_3$-$20ZnF_3$-$10YF_3$-$10ThF_4$
BIGaZYT2	$30BaF_2$-$12InF_3$-$18GaF_3$-$20ZnF_3$-$10YF_3$-$10ThF_4$

IV. RESULTS AND DISCUSSION

A. Excitation spectra

As an example, Fig. 1 shows the excitation spectra (at 4.2 K) of the $^4T_2\rightarrow{}^4A_2$ transition of the ZBLAN and BIGaZYT1 samples. All the spectra show a dip around 15 385 cm^{-1} (650 nm) which corresponds to the spin-forbidden transition $^4A_2\rightarrow{}^2E$. The other spin-forbidden transition $^4A_2\rightarrow{}^2T_1$ cannot be observed due to the narrow spectral range of the excitation wavelengths provided by the DCM dye. Figures 1(a) and 1(c) present the excitation spectra at a time delay of 1 μs for luminescence

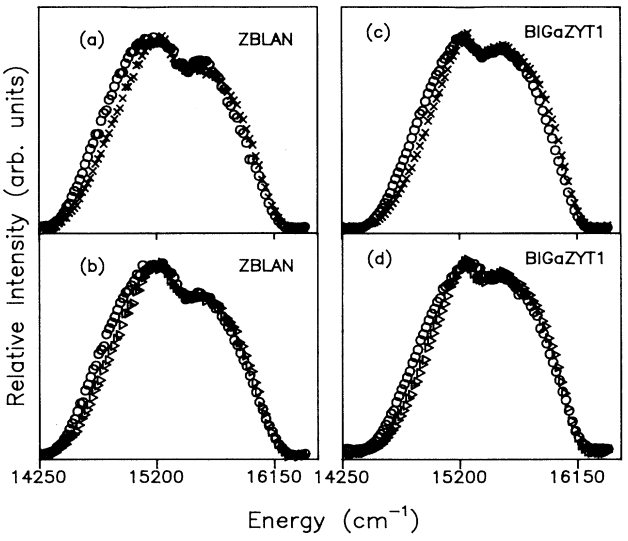

FIG. 1. Excitation spectra (at 4.2 K) of the $^4T_2\rightarrow{}^4A_2$ transition of the ZBLAN and BIGaZYT1 samples. (a) and (c) present the excitation spectra at a time delay of 1 μs for luminescence monitored at 750 nm (×) (at the high-energy side of the emission band) and at 890 nm (○) (at the peak position of the emission band). (b) shows the excitation spectra performed at 1 μs (○) and 300 μs (△), for luminescence monitored at 890 nm. (d) shows the excitation spectra performed at 1 μs (○) and 250 μs (△), for luminescence monitored at 890 nm. All the spectra show a dip around 15 385 cm^{-1} (650 nm) which corresponds to the spin-forbidden transition $^4A_2\rightarrow{}^2E$.

monitored at 750 nm (at the high-energy side of the emission band) and at 890 nm (at the peak position of the emission band).[7–9] As is easily seen, the high-energy spectra are blue shifted (≈ 50 cm^{-1}) as corresponds to the emission from high-energy sites. A red shift of the excitation spectra monitored at 1100 nm (at the low-energy side of the emission band) was also observed but is not shown here. Figures 1(b) and 1(d) show the excitation spectra performed at two time delays (1 and 300 μs for ZBLAN, and 1 and 250 μs for BIGaZYT1) for luminescence monitored at 890 nm. The blue shift of the excitation band monitored at high time delay corresponds to the emission losses from the low-field sites (sites of lower energy).

The observed antiresonance profiles of the excitation spectra have been analyzed in terms of the ratio $R(E)$ given by Eq. (1). As an example, Fig. 2 shows the analysis performed for the ZBLAN sample with the excitation spectrum obtained at 300 μs ($\lambda_{em}=890$ nm). In this case, as in Ref. 16 for absorption spectra, and due to the existence of two statistical site distributions of Cr^{3+} ions,[7–9] the background profile was obtained by fitting the excitation band in the wings to a double-Gaussian function. This fit can be seen in Fig. 2(a). The ratio $R(E)$ obtained experimentally and its fit to Eq. (1) are shown in Fig. 2(b). On the top of Fig. 3 we can see the antiresonance curves of the ZBLAN sample obtained at 1-μs monitoring at $\lambda_{em}=750$, 890, and 1100 nm. In the bottom of Fig. 3, the antiresonance curves are plotted for excitation spectra performed at two time delays (1 and 300 μs) monitored at 890 nm. The results obtained with the best fits of excitation spectra performed at three emission wavelengths (750, 890, 1100 nm) and at two time delays (1 μs, 250–300 μs) are listed in Table II for all samples. The following comments on the results can be made.

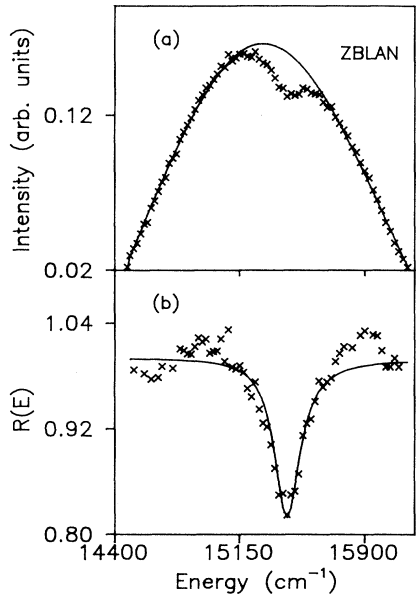

FIG. 2. Analysis of the excitation spectrum at 300 μs ($\lambda_{em}=890$ nm), performed in the ZBLAN sample. The background profile was obtained by fitting the excitation band to a double-Gaussian function. (a) Solid line, double-Gaussian fit; (×), excitation spectrum. (b) (×), ratio $R(E)$ obtained from (a); solid line, fit of $R(E)$ to Eq. (1).

(1) A pronounced blue shift of resonance energy (E_r) with decreasing λ_{em} and increasing time after excitation can be observed. This relevant behavior is closely related to glass inhomogeneity and means that the resonance energy shift due to interaction of sharp level ^2E with the

TABLE II. Parameters of ^2E antiresonance obtained from TR excitation spectra at 4.2 K corresponding to several HMFG. τ is the lifetime of the sharp state against decay to the continuum. The units of γ, E_r, and ξ' are cm^{-1}. τ is expressed in fs.

	(nm)	ρ^2	q	γ	E_r	τ	ξ'
ZBLAN							
($\tau=1$ μs)	$\lambda_{em}=750$	0.20	−0.018	101	15447	26	154
	$\lambda_{em}=890$	0.19	+0.064	94	15442	28	145
	$\lambda_{em}=1100$	0.13	−0.032	92	15335	29	145
($\tau=300$ μs)	$\lambda_{em}=890$	0.18	−0.031	93	15429	28	152
BIZYT							
($\tau=1$ μs)	$\lambda_{em}=750$	0.19	−0.086	128	15437	21	167
	$\lambda_{em}=890$	0.17	−0.084	107	15394	25	145
	$\lambda_{em}=1100$	0.13	+0.014	105	15357	25	141
($\tau=250$ μs)	$\lambda_{em}=890$	0.15	−0.064	99	15443	27	138
BIGaZYT1							
($\tau=1$ μs)	$\lambda_{em}=750$	0.19	−0.050	121	15443	22	168
	$\lambda_{em}=890$	0.15	+0.007	93	15414	28	139
	$\lambda_{em}=1100$	0.12	−0.073	83	15338	32	133
($\tau=250$ μs)	$\lambda_{em}=890$	0.12	+0.034	93	15460	28	145
BIGaZYT2							
($\tau=1$ μs)	$\lambda_{em}=750$	0.22	−0.037	123	15441	21	168
	$\lambda_{em}=890$	0.18	−0.071	85	15383	31	131
	$\lambda_{em}=1100$	0.17	−0.013	86	15351	31	134
($\tau=250$ μs)	$\lambda_{em}=890$	0.18	+0.045	100	15441	26	151

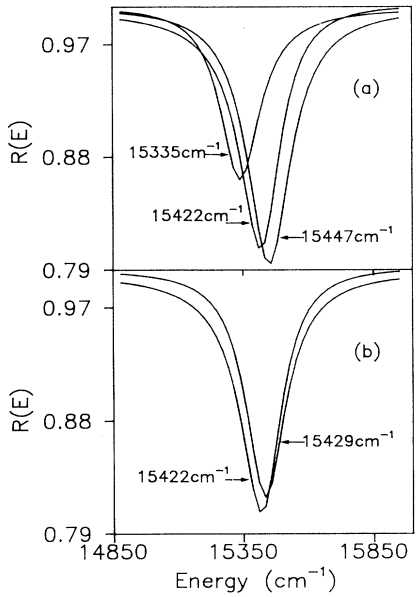

FIG. 3. ZBLAN antiresonance curves for the ^2E state, obtained (a) from the excitation spectra performed at 1 μs. λ_{em}=750, 890, and 1100 nm corresponding to resonance energies of 15 447, 15 422, and 15 335 cm^{-1}, respectively. (b) Obtained from the excitation spectra obtained at two time delays, monitored at 890 nm. 1 and 300 μs correspond to 15 422- and 15 429-cm^{-1} resonance energies, respectively.

$^4T_2$ continuum depends on the inhomogeneous broadening related with the Cr^{3+} ion site distributions.

(2) The ρ^2 values decrease substantially when λ_{em} changes from 750 to 1100 nm. The same behavior can be observed when increasing the time delay. As ρ^2 determines the fraction of band states that take part in the interference processes, it can be concluded that this fraction decreases when the Cr^{3+} ions emission shifts from high-energy sites to low-energy sites.

(3) Values obtained for q are low in all cases. This means that absorption antiresonances are produced by a sharp forbidden transition overlapping with a broad allowed transition. Due to the narrow spectral range of excitation wavelength, the values for q are somewhat uncertain, so no clear explanation for the variation of q can be given.

(4) We have calculated the one-electron spin-orbit coupling parameter ξ' from the observed value of the antiresonance linewidth[19] (γ). The obtained values are listed in Table II. These are, as expected, smaller than the free-ion value of 292-cm^{-1} (Ref. 24). The observed dispersion for obtained ξ' values can be attributed to the inhomogeneous broadening, as Lempicki *et al.* predicted for Cr^{3+} in nonfluoride glasses.[20]

(5) We have performed TR excitation spectra at liquid-nitrogen temperature (LNT) monitoring at the same λ_{em} as before. Although similar variations of resonance energies are observed, the evolution of parameter ρ^2 with increasing λ_{em} is not the same as at 4.2 K. The variation of ρ^2 is now smaller (ρ^2=0.17 at 750 and 890 nm and ρ^2=0.16 at 1100 nm for the ZBLAN sample). This behavior can be attributed to the vibrational broadening of the continuum states at temperatures above 4.2 K. The spectral widths γ, related to the finite lifetime of the ^2E discrete state due to configuration interaction, are slightly higher than those given in Table II at 4.2 K. This increase is due to decay processes which appear at higher temperatures.

B. Absorption spectra

The previous results demonstrate the influence of glass inhomogeneity on the antiresonance profiles in the excitation spectra of Cr^{3+} in HMFG. In this section, we analyze the influence of glass inhomogeneity on the antiresonance line profile of the absorption spectra given in Fig. 4 for the six samples studied. To perform this analysis, we have used the Fano theory adapted by Sturge, Guggenheim, and Pryce,[19] where the values for q can be calculated in an independent way from Eq. (5). In estimating q, we have taken a single- and a double-Gaussian function for the background spectrum:

$$G_2(E)=\exp\left[-\left[\frac{E-E_{\text{abs}}}{\sigma}\right]^2\right], \tag{6}$$

$$G_2(E)=\rho_1\exp\left[-\left[\frac{E-E_1}{\sigma_1}\right]^2\right]+\rho_2\exp\left[-\left[\frac{E-E_2}{\sigma_2}\right]^2\right], \tag{7}$$

where E_{abs}, E_1, E_2 are the Gaussian peak positions and σ, σ_1, σ_2 are the half-widths multiplied by $\sqrt{2}$. The Hil-

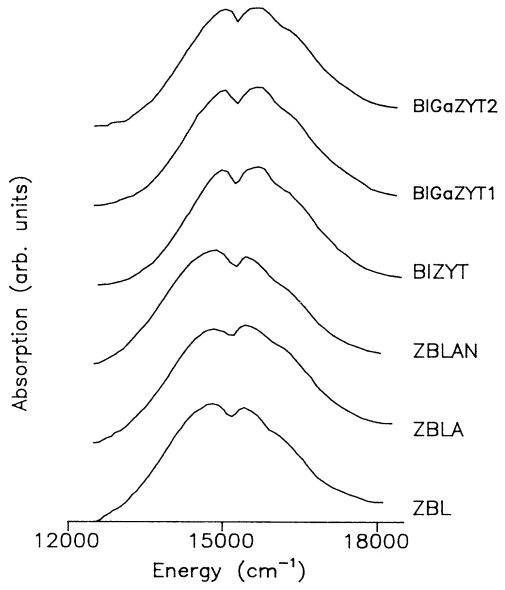

FIG. 4. Long-wavelength absorption band of Cr^{3+}-doped fluoride glasses at liquid-nitrogen temperature.

TABLE III. q values calculated from Eq. (5) for all samples taking for the background absorption spectra a single- and a double-Gaussian function. The observed q values (q_{obs}) were obtained from Ref. 16.

	q_{obs}	$q_{cal}(1)$	$q_{cal}(2)$	q_{obs}-$q_{cal}(1)$	q_{obs}-$q_{cal}(2)$
ZBL	−0.0055	+0.038	+0.055	−0.043	−0.060
BZLA	−0.085	−0.057	−0.034	−0.028	−0.051
ZBLAN	+0.11	+0.048	+0.087	+0.062	+0.023
BIZYT	−0.17	−0.21	−0.17	+0.040	0
BIGaZYT1	−0.105	−0.19	−0.17	+0.085	+0.065
BIGaZYT2	−0.145	−0.20	−0.18	+0.055	+0.035

bert transforms of $G_2(E)$ are found by numerical integration of Eqs. (6) and (7). As an example, Figs. 5(a) and 5(b) show the results obtained for given values of the background parameters belonging to the BIZYT sample. In Fig. 5(a), the fitting to the experimental absorption background was performed with a single Gaussian, whereas in Fig. 5(b) the fitting was made by a double-Gaussian function.

General expressions for q as a function of the background parameters (E_{abs},σ), and ($E_1,E_2,\sigma_1,\sigma_2,\rho_1/\rho_2$) for a single and double Gaussian, respectively, have been worked out. The expressions are

$$q(E_{abs},\sigma)=\frac{2}{\sqrt{\pi}}\int_0^{[(E_0-E_{abs})/\sigma]}\exp(t^2)dt\ , \tag{8}$$

$$q\left[E_1,E_2,\sigma_1,\sigma_2,\frac{\rho_1}{\rho_2}\right]=\frac{2}{\sqrt{\pi}}\left\{\frac{\rho_1}{\rho_2}\exp\left[-\left[\frac{E_0-E_1}{\sigma_1}\right]^2\right]+\exp\left[-\left[\frac{E_0-E_2}{\sigma_2}\right]^2\right]\right\}^{-1}$$
$$\times\left\{\frac{\rho_1}{\rho_2}\exp\left[-\left[\frac{E_0-E_1}{\sigma_1}\right]^2\right]\int_0^{[(E_0-E_1)/\sigma_1]}\exp(t^2)dt\right.$$
$$\left.+\exp\left[-\left[\frac{E_0-E_2}{\sigma_2}\right]^2\right]\int_0^{[(E_0-E_2)/\sigma_2]}\exp(t^2)dt\right\}. \tag{9}$$

Figure 6 shows the family of curves resulting from Eq. (8) for different values of σ and E_{abs}, taking a fixed value of 15 227 cm^{-1} for E_0. The dots are observed q values (q_{obs}) for fluoride glasses[16] plotted as a function of E_{abs} (roughly represented by the crystal-field parameter $10Dq$). The triangles are q values calculated from Eq. (8). A qualitatively good agreement can be observed for the two HMFG families studied in this work. The samples based on zirconium fluoride, which have a lower crystal field, present higher q values, whereas the barium-fluoride-based samples (higher Dq) have lower values for q. A discrepancy of about 20% is found between the theoreti-

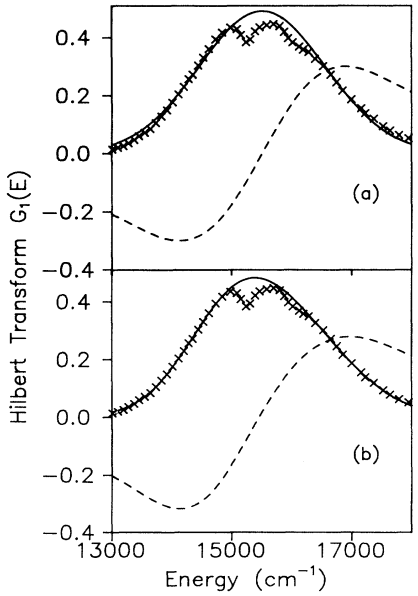

FIG. 5. (a) Solid line, single-Gaussian fit to the experimental absorption band ($\times$). Dashed line, $G_1(E)$ obtained by the Hilbert transform of Eq. (6). (b) Solid line, double-Gaussian fit to the experimental absorption band ($\times$). Dashed line, $G_1(E)$ obtained by the Hilbert transform of Eq. (7).

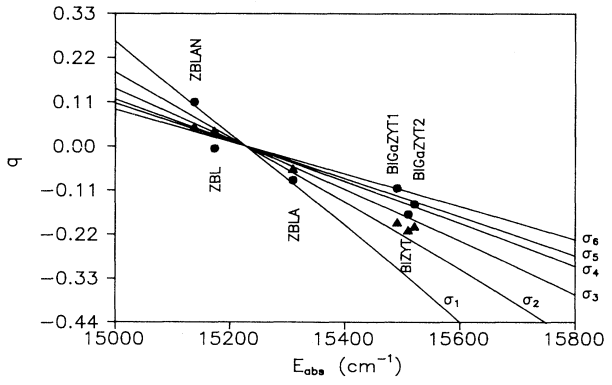

FIG. 6. Family of curves resulting from Eq. (8) for different values of σ and E_{abs}, taking a fixed value of 15 227 cm^{-1} for E_0. The dots are observed q values (q_{obs}) plotted as a function of E_{abs} (roughly represented by the crystal-field parameter $10Dq$) for the six fluoride glasses studied. The triangles are the calculated q values from Eq. (8). The values of σ are $\sigma_1=1000$ cm^{-1}, $\sigma_2=1400$ cm^{-1}, $\sigma_3=1800$ cm^{-1}, $\sigma_4=2200$ cm^{-1}, $\sigma_5=2400$ cm^{-1}, and $\sigma_6=2800$ cm^{-1}.

TABLE IV. Parameters of ^2E antiresonance obtained from the absorption spectra in HMFG at LNT. In this table the half-width of emission spectra, obtained by exciting at the peak position of the $^4A_2 \rightarrow {}^4T_2$ absorption band, is also included.

	ρ^2	q_{obs}	γ (cm^{-1})	E_r (cm^{-1})	E_{abs} (cm^{-1})	σ_{em} (cm^{-1})
ZBL	0.18	−0.055	238	15 245	15 173	935
ZBLA	0.19	−0.085	281	15 199	15 310	981
ZBLAN	0.17	0.110	170	15 238	15 161	932
BIZYT	0.20	−0.170	143	15 227	15 510	1024
BIGaZYT1	0.22	−0.105	214	15 245	15 491	1028
BIGaZYT2	0.19	−0.145	228	15 257	15 521	1032

cal σ values which correspond to represented dots and those obtained experimentally by fitting the background absorption spectra to a simple Gaussian function. Nevertheless, this disagreement may be justified by the inherent errors in the calculation of q as can also be observed in Table III. Moreover, the inhomogeneous broadening of the resonance profile can also contribute to the inaccuracy of the obtained values.

Table III shows the q values calculated from Eq. (5) for all samples taking for the background absorption spectra a single- and a double-Gaussian function. Agreement between the q_{obs} values and the q values calculated with a double Gaussian $G_2(E)$ [$q_{cal}(2)$] is slightly better than those calculated with $G_2(E)$ as a single Gaussian [$q_{cal}(1)$]. This discrepancy can also be appreciated in Fig. 5.

V. CONCLUSIONS

From the above results the following conclusions can be reached.

(i) The analysis of the antiresonance features which appear in the TR excitation spectra of Cr^{3+} in HMFG based on the Fano theory demonstrates the influence of glass inhomogeneity on the parameters related to the antiresonance profile. In particular, as Cr^{3+} ion emission varies from high-energy sites to low-energy sites, the resonance energy (E_r) is red shifted and the fraction of band states involved in the interference processes (ρ^2) decreases.

(ii) The small values obtained for q (in the excitation and absorption spectra) indicate that the antiresonances are produced by a sharp forbidden transition overlapping with a broad allowed transition.

(iii) The values obtained for ρ^2 (in the excitation and absorption spectra) are larger than the values given for crystals[20] and can be related to a larger disorder in glasses, which produces a more complete mixing of the spin-orbit components of level $^4T_2$ with components of level ^2E. If we compare the values of ρ^2, in Table IV, taken from the absorption spectra of the two families of HMFG, it can be seen that the fluorozirconate glasses have slightly smaller values of ρ^2 than the barium fluoride glasses and consequently are the most ordered glasses of the two families of HMFG. This result agrees with the conclusions obtained by Bendow *et al.*[25] by analyzing the polarized Raman scattering in different families of HMFG, and by the authors using TR spectroscopy.[7–9] Nevertheless, the ρ^2 values given by the excitation spectra show nearly opposite behavior. This fact can be understood because, in this case, only a reduced distribution of Cr^{3+} centers is selectively chosen, and therefore we lose information about the whole inhomogeneous broadening related with the Cr^{3+} site distribution.

(iv) As shown in Tables II and IV, the values of the antiresonance linewidths γ are influenced by the glass inhomogeneous broadening. Moreover, the half-widths of the ^2E antiresonance are correlated with the values of the emission half-width σ_{em}, in Table IV, obtained by exciting at the peak of the $^4A_2 \rightarrow {}^4T_2$ absorption band.

(v) Finally, the values for q (e.g., the numerical index which characterizes the line profile) strongly depend on background parameters which are related to the inhomogeneous broadening induced by changes in the glass composition. The dependence of the Fano antiresonance profile (in the absorption spectra) with these parameters has been studied for two families of HMFG and a qualitative agreement between experimental and calculated values was found.

ACKNOWLEDGMENTS

This work was supported by the Comisión Interministerial de Ciencia y Tecnología (CICYT) of the Spanish Government (Ref. No. 0188/89), and Basque Country Government (Ref. No. PGV 9012).

[1]T. Bates, in *Modern Aspects of the Vitreous State,* edited by J. D. Macken (Butterworth, London, 1962), Vol. 2, Chap. 5.
[2]C. R. Bamford, Phys. Chem. Glasses **3**, 189 (1962).
[3]S. A. Brawer and W. B. White, J. Chem. Phys. **67**, 2043 (1977).
[4]L. J. Andrews, A. Lempicki, and B. C. McCollum, J. Chem. Phys. **74**, 5526 (1981).
[5]P. T. Kenyon, L. J. Andrews, B. C. McCollum, and A. Lempicki, IEEE J. Quantum Electron. **QE-18**, 1189 (1982).
[6]R. Reisfeld, Mater. Sci. Eng. **71**, 375 (1985).
[7]R. Balda, J. Fernández, M. A. Illarramendi, M. A. Arriandia-

ga, J. Lucas, and J. L. Adam, Phys. Rev. B **44**, 4759 (1991).
[8]M. A. Illarramendi, J. Fernández, R. Balda, J. Lucas, and J. L. Adam, J. Lumin. **47**, 207 (1991).
[9]J. Fernández, M. A. Illarramendi, R. Balda, M. A. Arriandiaga, J. Lucas, and J. L. Adam, J. Non-Cryst. Solids **131-133**, 1230 (1991).
[10]R. Balda, J. Fernández, M. J. Elejalde, M. A. Illarramendi, and C. Jacoboni, J. Phys. Condens. Matter **3**, 7695 (1991).
[11]W. M. Yen, in *Optical Spectroscopoy of Glasses,* edited by I. Zschokke (Reidel, Dordrecht, 1986).
[12]R. E. Tischer, J. Chem. Phys. **48**, 4291 (1968).
[13]L. L. Lohr, J. Chem. Phys. **50**, 4596 (1969).
[14]G. O. Karapetyan, S. G. Lunter, and D. M. Yudin, Opt. Spectrosc. **14**, 370 (1963).
[15]H. L. Schlafer, H. Gausmann, and H. Witzke, J. Chem. Phys. **46**, 1423 (1967).
[16]M. A. Illarramendi, J. Fernández, and R. Balda, J. Lumin **53**, 461 (1992).
[17]U. Fano, Phys. Rev. **124**, 1866 (1961).
[18]U. Fano and J. W. Cooper, Phys. Rev. **137**, A1364 (1965).
[19]M. D. Sturge, H. J. Guggenheim, and M. H. L. Pryce, Phys. Rev. B **2**, 2459 (1970).
[20]A. Lempicki, L. Andrews, S. J. Nettel, B. C. McCollum, and E. I. Solomon, Phys. Rev. Lett. **44**, 1234 (1980).
[21]A. Meijerink and G. Blasse, Phys. Rev. B **40**, 7288 (1989).
[22]A. Lecoq and M. Poulain, Verres Réfract. **34**, 333 (1980).
[23]M. G. Drexhage, in *Treatise on Materials Science and Technology,* edited by M. Tomozawa and R. H. Doremus (Academic, New York, 1985), Vol. 26, pp. 151–243.
[24]M. Blume and R. Watson, Proc. R. Soc. London, Ser. A **271**, 563 (1963).
[25]B. Bendow *et al.*, J. Am. Ceram. Soc. **68**, C92 (1985).